

DEVELOPMENT AND CONVERGENCE ANALYSIS OF A FINITE VOLUME SCHEME FOR SOLVING BREAKAGE EQUATION*

JITENDRA KUMAR[†], JITRAJ SAHA[†], AND EVANGELOS TSOTSAS[‡]

Abstract. In this paper, we develop a new discretization method based on a finite volume approach for solving the breakage population balance equation. The scheme is designed to conserve the total mass of the system, and predict the total number of particles as well as the complete particle size distribution very accurately. The new method is computationally very efficient, easy to code, and robust to apply on uniform and nonuniform meshes. Development of the method is completed by providing a detailed mathematical analysis that includes consistency and convergence of the numerical solution. It is proved that the scheme is second order convergent independently of the type of mesh. Moreover, numerical results are compared against several test cases, including analytically tractable and practically oriented problems. It is found that the new method predicts the complete particle size distribution and its moments with high accuracy. The mathematical results of convergence analysis are also validated numerically.

Key words. population balance equation, breakage, finite volume scheme, nonuniform meshes, convergence analysis

AMS subject classifications. 65R20, 82C05

DOI. 10.1137/140980247

1. Introduction. The dynamic process by which particles undergo changes in their physical properties is called a *particulate process*. The study of particulate processes is a well-known subject in various branches of engineering, physics, chemistry, astrophysics, and in many more related areas. During the process, spontaneous collisions between the particles often cause changes in their mass, shape, size, volume, etc. The two best known particulate processes are aggregation and breakage. Aggregation is a process in which two or more particles unite to form a bigger particle. Breakage is the reverse process of aggregation. Thus, in a breakage event an agglomerate disintegrates into two or more smaller particles. In this work we are mainly concerned with the breakage or fragmentation process.

To study the change of the particle number density $f(x, t) \geq 0$, for particles of size (volume) $x \geq 0$ at time $t \geq 0$ in a physical system undergoing a breakage process, the following mathematical model known as the *population balance equation* (PBE) is required:

$$(1.1) \quad \frac{\partial f(x, t)}{\partial t} = \int_x^\infty b(x, \epsilon) S(\epsilon) f(\epsilon, t) d\epsilon - S(x) f(x, t)$$

subject to the initial condition

$$(1.2) \quad f(x, 0) = f_0(x) \geq 0.$$

*Received by the editors July 31, 2014; accepted for publication (in revised form) April 21, 2015; published electronically July 14, 2015. Alphabetical convention of authorship has been considered. The research of the authors was supported by Deutscher Akademischer Austausch Dienst (DAAD) (research fellowship of Jitraj Saha) and Alexander von Humboldt (AvH) Foundation (research fellowship of Jitendra Kumar).

<http://www.siam.org/journals/sinum/53-4/98024.html>

[†]Department of Mathematics, Indian Institute of Technology Kharagpur, Kharagpur-721302, India (jkumar@maths.iitkgp.ernet.in, jitraj@iitkgp.ac.in).

[‡]Chair of Thermal Process Engineering, Otto-von-Guericke University, D-39106 Magdeburg, Germany (evangelos.tsotsas@ovgu.de).

Without loss of generality, the time variable t and the size x are considered as dimensionless (Ramkrishna [15]). The selection function $S(x)$ denotes the rate at which particles of size x are selected to break into smaller fragments. The breakage function $b(x, \epsilon)$ is the probability density function denoting the formation of particles of size x due to the breakage of particles of size ϵ . Note that the selection function and breakage function may depend on time t but, for the sake of simplicity, we consider them independent of time. However, the time dependency of these functions does not add any further difficulties to the analysis performed in this work.

The breakage function is considered to satisfy the following conditions:

$$(1.3) \quad \int_0^y b(x, y) dx = \nu(y) \quad \forall y > 0, \quad b(x, y) = 0 \quad \forall x \geq y,$$

and

$$(1.4) \quad \int_0^y xb(x, y) dx = y \quad \forall y > 0.$$

The function $\nu(y)$ in (1.3), represents the total number of fragments in which the particle of size y splits up during the breakage process and, trivially, $\nu(y) \geq 1$. In general, when a particle of mass y breaks into smaller fragments then the total mass of the fragments formed is equal to y . This fact is captured by (1.4). Moreover, for a system that conserves the total mass during the fragmentation process, the breakage function $b(x, y)$ is considered to follow (1.4).

We shall now briefly explain different terms of (1.1). The left-hand side term describes the temporal rate of change of the particle number density. The first term on the right-hand side of (1.1) is called the birth term because it expresses the addition of particles of size x in the system due to the breakage of the bigger particles of size y . The second term is called the death term as it removes the particles of size x due to their breakage into smaller fragments.

Besides predicting the particle size distribution, estimation of moments of the distribution is also of great interest in several applications. Moments are integral properties of the distribution and some of them represent physical quantities that are easy to measure experimentally. Moreover, assessment of different numerical methods is usually based on their accuracy and efficiency to produce the particle size distribution as well as its moments. To this end, it is therefore important to formally define the j th moment of the particle size distribution as

$$(1.5) \quad \mu_j(t) = \int_0^\infty x^j f(t, x) dx.$$

The zeroth and first moments are proportional to the total number and total mass of the particles in the system at time t , respectively. It is easy to show for a wide class of breakage and selection functions that the PBE (1.1) satisfies the following equations for the first two moments:

$$(1.6) \quad \frac{d\mu_0}{dt} = \int_0^\infty S(x) f(x, t) [\nu(x) - 1] dx$$

and

$$(1.7) \quad \frac{d\mu_1}{dt} = 0.$$

Equation (1.6) models the temporal change of the zeroth moment and it can only be written in a closed form of moments for some special breakage and selection

functions. Equation (1.7) shows the mass conservation property of the population balance model.

As pointed out above, the PBE is a mass conservation law written for number density function f . Therefore, it is interesting to note that the above PBE (1.1) can be written in the so called *mass conserving form* as

$$(1.8) \quad \frac{x\partial f(x,t)}{\partial t} = \frac{\partial}{\partial x} \left[\int_x^\infty \int_0^x ub(u,v)S(v)f(t,v) du dv \right].$$

For the detailed derivation of the above equation, readers are referred to Kumar and Kumar [9]. This form is specially useful for applying a finite volume scheme because of a natural feature of the scheme to conserve mass when applied to the conservation law in the mass conserving form such as (1.8). In other words, a finite volume scheme automatically conserves mass when applied to a mass conservation law written in the form of (1.8).

The mathematical results on the existence and uniqueness of the solution of (1.1) can be found in [3, 10, 11, 13, 14, 16]. In these studies, the authors have mainly developed the existence and uniqueness theory by considering the solutions in different spaces with suitable bounds over the selection and breakage functions. But it has been seen in the articles [2, 18, 19] that (1.1) can be solved analytically only for some simple forms of the selection and breakage functions. This situation has led to the requirement of numerical methods to solve the PBEs.

In (1.1), we find that the range of the volume variable x varies from 0 to ∞ . However, for numerical treatments it is necessary to fix a finite range for the computational domain. Let us fix the computational domain to $(0, x_{\max}]$, where $0 < x_{\max} < \infty$. Hence, for $x \in (0, x_{\max}]$ and time $t \in (0, T]$, $T < \infty$, the truncated forms of the breakage PBE (1.1) and initial condition (1.2) are given as

$$(1.9) \quad \frac{\partial f(x,t)}{\partial t} = \int_x^{x_{\max}} b(x,\epsilon)S(\epsilon)f(\epsilon,t) d\epsilon - S(x)f(x,t)$$

and

$$(1.10) \quad f(x,0) = f_0(x), \quad x \in (0, x_{\max}].$$

Similarly, infinity in the mass conserving form (1.8) needs to be replaced by x_{\max} for its numerical applicability.

2. State of the art. The numerical methods are mainly stochastic methods, finite volume methods, moment methods, asymptotic solution techniques, sectional methods, etc. Our focus in this paper is to explore the existing finite volume methods and develop a new finite volume approach for solving breakage PBE. Let us first review the existing literature on the development and analysis of different numerical schemes. Several researchers have applied the finite volume method to approximate pure aggregation, pure breakage, and coupled aggregation-breakage PBEs. Besides developing and validating the numerical schemes, convergence and stability analysis have also been studied widely.

Let us begin with the work of Filbet and Laurençot [4]. The authors in [4] have proposed a finite volume approximation of the mass conservation form of the pure aggregation equation. Later Bourgade and Filbet [1] have extended the idea of Filbet and Laurençot [4] by considering the mass conservation form of the coupled

binary aggregation and binary fragmentation PBEs. A detailed consistency and stability analysis of the numerical scheme has also been provided in [1] where both the aggregation and breakage kernels have been chosen from the space $L_{loc}^\infty(\mathbb{R}^+ \times \mathbb{R}^+)$, $\mathbb{R}^+ = (0, \infty)$.

Sectional methods belong to another popular category of solution techniques. These methods are well known for predicting particle size distribution and its moments accurately on coarse meshes. In [7, 8], Kumar and Warnecke have studied the convergence and stability of two well known sectional methods, the fixed pivot technique and the cell average technique, for pure breakage problems. The breakage kernels S and b are taken from the space of twice continuously differentiable functions. It is seen that the convergence rates of the fixed pivot and cell average techniques depend on the type of meshes. It is found there that the fixed pivot technique does not converge on certain nonuniform meshes while the cell average technique is only first order accurate on those meshes. These aspects may be taken as their weak points.

The work of Forestier-Coste and Mancini [5] is different from the previous ones. They proposed for pure aggregation a new numerical approximation by applying a finite volume approach directly to the standard form of aggregation PBE. The authors modified the kernel to conserve the total mass of the system in numerical calculations.

Following Filbet and Laurençot [4], Kumar and Kumar [9] have recently developed a finite volume scheme approximating the mass conservation form of the pure multiple fragmentation equation (1.8). Interestingly, the authors have proved the second order convergence of the method independently of the meshes. Let us briefly describe their formulation and analyze its features. As usual, the method relies on discretizing the computational domain $(0, x_{\max}]$ into I number of small cells $(x_{i-1/2}, x_{i+1/2}]$, $i = 1, \dots, I$, with $x_{1/2} = 0$ and $x_{I+1/2} = x_{\max}$. The width of the i th cell is denoted by Δx_i , i.e., $\Delta x_i = x_{i+1/2} - x_{i-1/2}$. The representative or the grid point of the i th cell, denoted by x_i , is given as the mean of the cell, i.e., $x_i = (x_{i-1/2} + x_{i+1/2})/2$.

Let f_i and g_i approximate the average value of the number densities and the mass in the i th cell, respectively, i.e.,

$$(2.1) \quad f_i \approx \frac{1}{\Delta x_i} \int_{x_{i-1/2}}^{x_{i+1/2}} f(x, t) dx, \quad g_i \approx \frac{1}{\Delta x_i} \int_{x_{i-1/2}}^{x_{i+1/2}} x f(x, t) dx.$$

The discrete formulation of Kumar and Kumar [9] reads as

$$(2.2) \quad \frac{dg_i}{dt} = -\frac{1}{\Delta x_i} (J_{i+1/2} - J_{i-1/2}),$$

where

$$(2.3) \quad J_{i+1/2} = - \sum_{k=i+1}^I g_k \int_{x_{k-1/2}}^{x_{k+1/2}} \frac{S(\epsilon)}{\epsilon} d\epsilon \int_0^{x_{i+1/2}} u b(u, x_k) du.$$

The number density f_i is calculated from the relation $g_i = f_i x_i$. Let us check the scheme of Kumar and Kumar [9] for a simple test problem of uniform breakage function $b(x, y) = 2/y$, linear selection function $S(x) = x$, and monodisperse particles of size unity as initial condition. The computational domain is taken as $[10^{-8}, 1]$ and discretized into 30 nonuniform cells of geometric type $x_{i+1/2} = rx_{i-1/2}$, $r > 1$. Due to the nature of the formation of the geometric grids, a nonzero left endpoint of the computational domain has been considered. For this type of problem, the particle population of smaller size particles (as a result of breakage, particle population

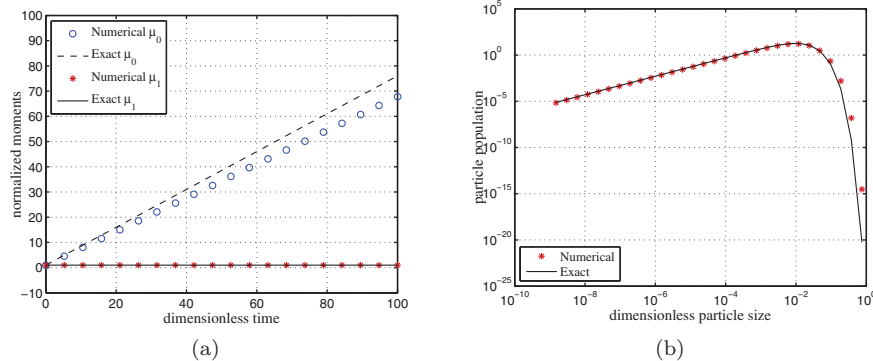


FIG. 1. A comparison of numerical results of Kumar and Kumar [9] with the exact solutions.

increases for smaller particles) is quite higher than the larger particles. Therefore, geometric grids are preferable as compared to uniform grids for such problems. This computation is performed until $t = 100$. The numerical results along with the exact solutions are plotted in Figure 1. As expected, the total mass of the particles remains conserved. However, the prediction of the zeroth moment is rather poor and a clear deviation from the true values is observed in Figure 1(a). Finally, in Figure 1(b), particle population of each cell is plotted against the representative size of the respective cell at the end time $t = 100$. A slight overprediction of particles at large sizes is observed. Nevertheless, particle population in most of the cells is well predicted by the method.

In this work, we propose a finite volume scheme that relies on the standard form of the PBE (1.9) rather than the form (1.8). A similar approach has been pursued in the work of Forestier-Coste and Mancini [5] for aggregation problems. The objective is to overcome the above illustrated weakness of a finite volume scheme to predict the zeroth moment accurately. Moreover, the method is expected to maintain simplicity of its mathematical formulation, conserve mass, and predict the complete size distribution precisely. A further aim is to complete the derivation of the method by providing its mathematical analysis including convergence and consistency.

The outline of this paper is as follows. In section 3, a new numerical method for solving the breakage PBE equation is derived and various interesting features of the method are discussed. Then, the convergence analysis of the proposed method is provided in section 4. The numerical results are verified in section 5 and, finally, some conclusions are drawn in section 6.

3. New formulation. We shall now proceed to develop a new finite volume scheme for solving the breakage PBE. Recall, $f_i(t)$ denotes the average number density of particles in the i th cell. Assuming sufficient smoothness of f , we also have

$$f_i(t) = f(x_i, t) + \mathcal{O}(\Delta x_i^2).$$

This implies that $f_i(t)$ and $f(x_i, t)$ are equal up to the order of Δx^2 . As pointed out earlier, we discretize the standard form of the PBE (1.9). So, integrating (1.9) over the cell Λ_i , we obtain

$$(3.1) \quad \frac{df_i}{dt} = B_i - D_i, \quad i = 1, \dots, I,$$

with the initial data

$$(3.2) \quad f_i(0) = \frac{1}{\Delta x_i} \int_{x_{i-1/2}}^{x_{i+1/2}} f_0(x) dx.$$

Here the birth terms B_i and the death terms D_i are given as

$$(3.3) \quad B_i = \frac{1}{\Delta x_i} \int_{x_{i-1/2}}^{x_{i+1/2}} \int_x^{x_{i+1/2}} b(x, \epsilon) S(\epsilon) f(\epsilon, t) d\epsilon dx$$

and

$$(3.4) \quad D_i = \frac{1}{\Delta x_i} \int_{x_{i-1/2}}^{x_{i+1/2}} S(x) f(x, t) dx.$$

To set up discrete equations we need to discretize the birth and death terms using suitable quadrature rules. In the general case of nonuniform mesh, we denote $\Delta x = \max_i \Delta x_i$, $\delta x = \min_i \Delta x_i$, and assume that there exists a positive constant K (independent of the mesh) such that

$$(3.5) \quad \frac{\Delta x}{\delta x} \leq K.$$

Let us first discretize the birth term as follows. Changing the order of integration in (3.3), we obtain

$$(3.6) \quad B_i = \frac{1}{\Delta x_i} \left[\int_{x_{i-1/2}}^{x_{i+1/2}} S(\epsilon) f(\epsilon) \int_{x_{i-1/2}}^{\epsilon} b(x, \epsilon) dx d\epsilon \right. \\ \left. + \sum_{k=i+1}^I \int_{x_{k-1/2}}^{x_{k+1/2}} S(\epsilon) f(\epsilon) \int_{x_{i-1/2}}^{x_{i+1/2}} b(x, \epsilon) dx d\epsilon \right].$$

Using the *midpoint approximation* for the outer integrals in both the right-hand side terms, we find

$$(3.7) \quad B_i = S_i f_i \int_{x_{i-1/2}}^{x_i} b(x, x_i) dx + \frac{1}{\Delta x_i} \sum_{k=i+1}^I S_k f_k \Delta x_k \int_{x_{i-1/2}}^{x_{i+1/2}} b(x, x_k) dx + \mathcal{O}(\Delta x^2).$$

Here $S_i = S(x_i)$. Combining the terms on the right-hand side, we obtain

$$(3.8) \quad B_i = \frac{1}{\Delta x_i} \sum_{k=i}^I S_k f_k \Delta x_k \int_{x_{i-1/2}}^{p_k^i} b(x, x_k) dx + \mathcal{O}(\Delta x^2),$$

where p_k^i is given as

$$p_k^i = \begin{cases} x_i & \text{when } k = i, \\ x_{i+1/2} & \text{otherwise.} \end{cases}$$

Proceeding similarly for the death term (3.4), we arrive at

$$(3.9) \quad D_i = S_i f_i + \mathcal{O}(\Delta x^2).$$

To this end, we can propose the following discrete equations for approximating the number density f_i . Let us denote the numerical approximation of f_i by \hat{f}_i , then we have

$$(3.10) \quad \frac{d\hat{f}_i}{dt} = \frac{1}{\Delta x_i} \sum_{k=i}^I S_k \hat{f}_k \Delta x_k \mathcal{B}_{ik} - S_i \hat{f}_i, \quad i = 1, \dots, I,$$

where

$$(3.11) \quad \mathcal{B}_{ik} = \int_{x_{i-1/2}}^{p_k^i} b(x, x_k) dx.$$

The initial condition is given from 3.2 as

$$(3.12) \quad \hat{f}_i(0) = f_i(0), \quad i = 1, \dots, I.$$

Theoretically, the above discrete equations can be used to approximate the number density function in different cells. However, we will show in the following proposition that the above discrete equations do not follow the law of conservation of mass.

PROPOSITION 3.1. *The discrete formulation (3.10) does not conserve the total volume or mass; that is,*

$$(3.13) \quad \frac{d}{dt} \sum_{i=1}^I (x_i \hat{f}_i \Delta x_i) \neq 0.$$

Proof. Let us multiply by x_i on both sides of (3.10) and then sum over i to get the rate of change of total mass as

$$(3.14) \quad \frac{d}{dt} \sum_{i=1}^I (x_i \hat{f}_i \Delta x_i) = \sum_{i=1}^I x_i \sum_{k=i}^I S_k \hat{f}_k \Delta x_k \mathcal{B}_{ik} - \sum_{i=1}^I x_i S_i \hat{f}_i \Delta x_i.$$

Changing the order of the sums leads to

$$(3.15) \quad \begin{aligned} \frac{d}{dt} \sum_{i=1}^I (x_i \hat{f}_i \Delta x_i) &= \sum_{k=1}^I S_k \hat{f}_k \Delta x_k \sum_{i=1}^k x_i \mathcal{B}_{ik} - \sum_{i=1}^I x_i S_i \hat{f}_i \Delta x_i \\ &= \sum_{k=1}^I S_k \hat{f}_k \Delta x_k \left[\sum_{i=1}^k x_i \mathcal{B}_{ik} - x_k \right]. \end{aligned}$$

Using the fact that $\int_0^{x_k} xb(x, x_k) dx = x_k$, we obtain

$$(3.16) \quad \frac{d}{dt} \sum_{i=1}^I (x_i \hat{f}_i \Delta x_i) = \sum_{k=1}^I S_k \hat{f}_k \Delta x_k \left[\sum_{i=1}^k x_i \int_{x_{i-1/2}}^{p_k^i} b(x, x_k) dx - \sum_{i=1}^k \int_{x_{i-1/2}}^{p_k^i} xb(x, x_k) dx \right].$$

One can clearly observe that

$$(3.17) \quad \frac{d}{dt} \sum_{i=1}^I (x_i \hat{f}_i \Delta x_i) = \sum_{k=1}^I S_k \hat{f}_k \Delta x_k \left[\sum_{i=1}^k \int_{x_{i-1/2}}^{p_k^i} b(x, x_k) (x_i - x) dx \right] \neq 0.$$

This proves that the total mass does not remain conserved in numerical results of the method (3.10). \square

Note that mass conservation is an essential property of any numerical scheme. On the one hand, the above discrete equations should not be used in computation. On the other hand, if we estimate the prediction of the zeroth moment using the above discrete equations we find that

$$(3.18) \quad \frac{d}{dt} \sum_{k=1}^I \hat{f}_i \Delta x_i = \sum_{k=1}^I S_k \hat{f}_k \Delta x_k [\nu(x_k) - 1].$$

It is to be noted that (3.18) is analogous to the continuous form (1.6). Thus using the fact that (3.18) is a natural discretization of (1.6), the discrete equations (3.10) are expected to predict the zeroth moment with high accuracy. The validity of this aspect will be shown later in numerical comparisons. We call a numerical scheme *consistent with respect to the zeroth moment* if it satisfies the property (3.18). So the objective is to modify the discrete equations (3.10) so that the total mass gets conserved without disturbing the rule (3.18).

To this end, we propose the following modified finite volume scheme as

$$(3.19) \quad \frac{d\hat{f}_i}{dt} = \frac{1}{\Delta x_i} \sum_{k=i}^I \omega_k^b S_k \hat{f}_k \Delta x_k \mathcal{B}_{ik} - \omega_i^d S_i \hat{f}_i$$

with the same initial condition (3.12) as above. Here ω_k^b and ω_k^d are the weights responsible for the scheme (3.19) to be mass conservative and consistent w.r.t. the zeroth moment. These weights are given as

$$(3.20) \quad \omega_k^b = \frac{x_k [\nu(x_k) - 1]}{\sum_{i=1}^{k-1} (x_k - x_i) \mathcal{B}_{ik}} \quad \text{and} \quad \omega_k^d = \frac{\omega_k^b}{x_k} \sum_{i=1}^k x_i \mathcal{B}_{ik}, \quad k = 2, \dots, I.$$

The values of ω_1^b and ω_1^d are taken to be zero.

Remark 1. The weights ω_k^b and ω_k^d are independent of the number density function and the breakage function has been assumed to be constant in time, therefore, they may be calculated prior to the computation of the system of differential equations (3.19). But in general, the breakage function is time dependent. In that case, the weights have to be calculated at each time step of the computation.

Next we will show that the new scheme conserves mass and is consistent w.r.t. the zeroth moment.

PROPOSITION 3.2. *The discrete formulation (3.19) of the continuous breakage PBE (1.9) conserves the total mass of the system and is consistent w.r.t. the zeroth moment.*

Proof. Multiplying the formulation (3.19) by x_i on both sides and then summing over i , we obtain

$$(3.21) \quad \frac{d}{dt} \sum_{i=1}^I (x_i \hat{f}_i \Delta x_i) = \sum_{k=1}^I S_k \hat{f}_k \Delta x_k \left[\omega_k^b \sum_{i=1}^k x_i \mathcal{B}_{ik} - \omega_k^d x_k \right].$$

Substituting the value of ω_k^d from (3.20) in the above equation, we get

$$(3.22) \quad \frac{d}{dt} \sum_{i=1}^I (x_i \hat{f}_i \Delta x_i) = \sum_{k=1}^I S_k \hat{f}_k \Delta x_k \omega_k^b \left[\sum_{i=1}^k x_i \mathcal{B}_{ik} - \sum_{i=1}^k x_i \mathcal{B}_{ik} \right] = 0.$$

This follows the mass conservation property. For the total number of particles, we calculate

$$(3.23) \quad \frac{d}{dt} \sum_{i=1}^I \hat{f}_i \Delta x_i = \sum_{k=1}^I S_k \hat{f}_k \Delta x_k \left[\omega_k^b \sum_{i=1}^k \mathcal{B}_{ik} - \omega_k^d \right].$$

The substitution of ω_k^d from (3.20) gives

$$\begin{aligned} \frac{d}{dt} \sum_{i=1}^I \hat{f}_i \Delta x_i &= \sum_{k=1}^I S_k \hat{f}_k \Delta x_k \omega_k^b \left[\sum_{i=1}^k \mathcal{B}_{ik} - \frac{1}{x_k} \sum_{i=1}^k x_i \mathcal{B}_{ik} \right] \\ &= \sum_{k=1}^I S_k \hat{f}_k \Delta x_k \omega_k^b \frac{1}{x_k} \sum_{i=1}^k (x_k - x_i) \mathcal{B}_{ik}. \end{aligned}$$

Finally, substituting ω_k^b from (3.20), we get

$$(3.24) \quad \frac{d}{dt} \sum_{i=1}^I \hat{f}_i \Delta x_i = \sum_{k=1}^I S_k \hat{f}_k \Delta x_k [\nu(x_k) - 1].$$

Comparing (3.24) and (3.18) it can be concluded that the new scheme is consistent w.r.t. the zeroth moment. \square

4. Convergence analysis. To perform convergence analysis, it is convenient to write the system of discrete equations in a vector form. Let \mathbf{f} and $\hat{\mathbf{f}}$ be vectors with components the true average values f_i and their numerical approximations \hat{f}_i , respectively. We write the discrete equations (3.19) in a vector form as

$$(4.1) \quad \frac{d\hat{\mathbf{f}}}{dt} = \mathbf{J}(\hat{\mathbf{f}}), \quad \hat{\mathbf{f}}(0) = \mathbf{f}(0),$$

where $\hat{\mathbf{B}}, \hat{\mathbf{D}}, \mathbf{J} \in \mathbb{R}^I$ are the functions of $\hat{\mathbf{f}}$ with the components

$$(4.2) \quad \hat{B}_i(\hat{\mathbf{f}}) = \frac{1}{\Delta x_i} \sum_{k=i}^I \omega_k^b S_k \hat{f}_k \Delta x_k \mathcal{B}_{ik},$$

$$(4.3) \quad \hat{D}_i(\hat{\mathbf{f}}) = \omega_i^d S_i \hat{f}_i,$$

$$(4.4) \quad J_i(\hat{\mathbf{f}}) = \hat{B}_i(\hat{\mathbf{f}}) - \hat{D}_i(\hat{\mathbf{f}}).$$

Before we proceed to discuss convergence of the semidiscrete system (4.1), we first assemble some useful theorems and definitions. Let us define the discrete L^1 norm on \mathbb{R}^I as

$$(4.5) \quad \|\mathbf{f}(t)\| = \sum_{i=1}^I |f_i(t)| \Delta x_i.$$

DEFINITION 1. *The spatial truncation error is defined as the residual left by substituting the exact solution $\mathbf{f} = [f_1(t), \dots, f_I(t)]$ into the discrete equations as*

$$(4.6) \quad \sigma(t) = \frac{d\mathbf{f}(t)}{dt} - \mathbf{J}(\mathbf{f}).$$

The scheme is called consistent of order p if, for $\Delta x \rightarrow 0$

$$(4.7) \quad \|\sigma(t)\| = \mathcal{O}(\Delta x^p) \text{ uniformly for all } t, 0 \leq t \leq T.$$

DEFINITION 2. The global discretization error is defined by $\epsilon(t) = \mathbf{f}(t) - \hat{\mathbf{f}}(t)$. The scheme is considered to be convergent of order p if, for $\Delta x \rightarrow 0$,

$$(4.8) \quad \|\epsilon(t)\| = \mathcal{O}(\Delta x^p) \text{ uniformly for all } t, 0 \leq t \leq T.$$

Before proceeding to the main result we review the following theorems.

THEOREM 4.1. Suppose that \mathbf{J} is continuous and satisfies the Lipschitz condition

$$(4.9) \quad \|\mathbf{J}(\mathbf{f}) - \mathbf{J}(\mathbf{g})\| \leq L \|\mathbf{f} - \mathbf{g}\| \text{ for all } \mathbf{f}, \mathbf{g} \in \mathbb{R}^I, L < \infty.$$

Then the solution of the semidiscrete system $\mathbf{f}' = \mathbf{J}(\mathbf{f})$ is nonnegative if and only if for any vector $\mathbf{f} \in \mathbb{R}^I$ and all $i = 1, 2, \dots, I$, and $t \geq 0$,

$$\mathbf{f} \geq 0, \quad f_i = 0 \Rightarrow J_i(\mathbf{f}) \geq 0.$$

Proof. The proof is given in Theorem 7.1, Chapter 1 of Hundsdorfer and Verwer [6]. \square

THEOREM 4.2. Let us assume that a Lipschitz condition on $\mathbf{J}(\mathbf{f})$ is satisfied for $0 \leq t \leq T$ and for all $\mathbf{f}, \hat{\mathbf{f}} \in \mathbb{R}^I$. That is, \mathbf{J} satisfies

$$(4.10) \quad \|\mathbf{J}(\mathbf{f}) - \mathbf{J}(\hat{\mathbf{f}})\| \leq L \|\mathbf{f} - \hat{\mathbf{f}}\|, \quad L < \infty.$$

Then a consistent discretization method is also convergent and the convergence order is the same as the order of the consistency.

Proof. A generalized version of this theorem is provided in Linz [12]. \square

PROPOSITION 4.3. Let us assume that the kernels S and b are twice continuously differentiable functions over $(0, x_{\max}]$ and $(0, x_{\max}] \times (0, x_{\max}]$, respectively, then there exists a constant

$$L = C \max_{x \in (0, x_{\max}]} [S(x)\nu(x)] < \infty, \quad \text{where } C > 0,$$

such that the Lipschitz condition on \mathbf{J} , i.e.,

$$\|\mathbf{J}(\mathbf{f}) - \mathbf{J}(\hat{\mathbf{f}})\| \leq L \|\mathbf{f} - \hat{\mathbf{f}}\| \text{ for all } \mathbf{f}, \hat{\mathbf{f}} \in \mathbb{R}^I$$

is satisfied.

Proof. Using the definition of the norm (4.5), we have

$$(4.11) \quad \|\mathbf{J}(\mathbf{f}) - \mathbf{J}(\hat{\mathbf{f}})\| = \sum_{i=1}^I |J_i(f_i) - J_i(\hat{f}_i)| \Delta x_i.$$

Substituting J_i from (4.4), we find

$$(4.12) \quad \|\mathbf{J}(\mathbf{f}) - \mathbf{J}(\hat{\mathbf{f}})\| = \sum_{i=1}^I \frac{1}{\Delta x_i} \left| \sum_{k=i}^I \omega_k^b S_k \mathcal{B}_{ik} (f_k - \hat{f}_k) \Delta x_k - \omega_i^d S_i (f_i - \hat{f}_i) \Delta x_i \right| \Delta x_i.$$

Further simplifications lead to

$$(4.13) \quad \left\| \mathbf{J}(\mathbf{f}) - \mathbf{J}(\hat{\mathbf{f}}) \right\| \leq \underbrace{\sum_{i=1}^I \sum_{k=i}^I \omega_k^b S_k \mathcal{B}_{ik} |f_k - \hat{f}_k| \Delta x_k}_{=:T_1} + \underbrace{\sum_{i=1}^I \omega_i^d S_i |f_i - \hat{f}_i| \Delta x_i}_{=:T_2}.$$

Let us simplify the first term on the right-hand side of the preceding equation. Changing the order of the summation of the term T_1 , we have

$$(4.14) \quad T_1 = \sum_{i=1}^I \sum_{k=i}^I \omega_k^b \mathcal{B}_{ik} S_k |f_k - \hat{f}_k| \Delta x_k = \sum_{k=1}^I \sum_{i=1}^k \omega_k^b \mathcal{B}_{ik} S_k |f_k - \hat{f}_k| \Delta x_k.$$

Using the definition of the weight ω_k^b from (3.20) and the fact that $\omega_1^b = 0$, the above relation is written as

$$\begin{aligned} T_1 &= \sum_{k=2}^I \sum_{i=1}^k \left[\frac{x_k \nu(x_k)}{\sum_{j=1}^k (x_k - x_j) \mathcal{B}_{jk}} - \frac{x_k}{\sum_{j=1}^k (x_k - x_j) \mathcal{B}_{jk}} \right] \mathcal{B}_{ik} S_k |f_k - \hat{f}_k| \Delta x_k \\ &= \sum_{k=2}^I \sum_{i=1}^k \left[\frac{\nu(x_k) (x_k - x_i)}{\sum_{j=1}^k (x_k - x_j) \mathcal{B}_{jk}} + \frac{x_i \nu(x_k)}{\sum_{j=1}^k (x_k - x_j) \mathcal{B}_{jk}} \right] \mathcal{B}_{ik} S_k |f_k - \hat{f}_k| \Delta x_k \\ &\quad - \sum_{k=2}^I \sum_{i=1}^k \frac{x_k}{\sum_{j=1}^k (x_k - x_j) \mathcal{B}_{jk}} \mathcal{B}_{ik} S_k |f_k - \hat{f}_k| \Delta x_k. \end{aligned}$$

This can be further simplified by using $\nu(x_k) = \sum_{i=1}^k \mathcal{B}_{ik}$ as

$$(4.15) \quad \begin{aligned} T_1 &= \sum_{k=2}^I \frac{\nu(x_k) S_k |f_k - \hat{f}_k| \Delta x_k}{\sum_{j=1}^k (x_k - x_j) \mathcal{B}_{jk}} \left[\sum_{i=1}^k (x_k - x_i) \mathcal{B}_{ik} + \sum_{i=1}^k x_i \mathcal{B}_{ik} \right] \\ &\quad - \sum_{k=2}^I \frac{x_k S_k |f_k - \hat{f}_k| \Delta x_k}{\sum_{j=1}^k (x_k - x_j) \mathcal{B}_{jk}} \nu(x_k). \end{aligned}$$

Rearranging the terms, we get

$$\begin{aligned} T_1 &= \sum_{k=2}^I \nu(x_k) S_k |f_k - \hat{f}_k| \Delta x_k + \sum_{k=2}^I \frac{\nu(x_k) S_k |f_k - \hat{f}_k| \Delta x_k}{\sum_{j=1}^k (x_k - x_j) \mathcal{B}_{jk}} \left[\sum_{i=1}^k x_i \mathcal{B}_{ik} - x_k \right] \\ &\leq \sum_{k=2}^I \nu(x_k) S_k |f_k - \hat{f}_k| \Delta x_k + \sum_{k=2}^I \frac{\nu(x_k) S_k |f_k - \hat{f}_k| \Delta x_k}{\sum_{j=1}^k (x_k - x_j) \mathcal{B}_{jk}} \left| \sum_{i=1}^k x_i \mathcal{B}_{ik} - x_k \right|. \end{aligned}$$

Since, $b(x, y)$ is a twice continuously differentiable function, by the application of the midpoint and the right end approximation of the integrals, we obtain

$$(4.16) \quad x_k = \int_0^{x_k} xb(x, x_k) dx = \sum_{j=1}^k \int_{x_{j-1/2}}^{p_k^j} xb(x, x_k) dx = \sum_{j=1}^k x_j \mathcal{B}_{jk} + \mathcal{O}(\Delta x)^2.$$

Hence,

$$(4.17) \quad \left| x_k - \sum_{j=1}^k x_j \mathcal{B}_{jk} \right| = \left| \mathcal{O}(\Delta x)^2 \right| \leq L_1 (\Delta x)^2, \quad \text{where } L_1 < \infty \text{ is constant.}$$

Moreover, for $k = 2, \dots, I$ we also have

$$(4.18) \quad \sum_{j=1}^{k-1} (x_k - x_j) \mathcal{B}_{jk} \geq (x_k - x_{k-1}) \sum_{i=1}^{k-1} \mathcal{B}_{ik} \geq \Delta x_k \left[\int_0^{x_{k-1}/2} b(x, x_k) dx \right] \geq L_2 (\delta x),$$

where L_2 is a constant, satisfying

$$0 < L_2 = \min_{k \in \{2, \dots, I\}} \left[\int_0^{x_{k-1}/2} b(x, x_k) dx \right].$$

Recalling the relation of T_1 and the relation (3.5), we find

$$\begin{aligned} T_1 &\leq \sum_{k=2}^I \nu(x_k) S_k |f_k - \hat{f}_k| \Delta x_k + \sum_{k=2}^I \frac{(\Delta x)^2}{\delta x} \frac{L_1}{L_2} \nu(x_k) S_k |f_k - \hat{f}_k| \Delta x_k \\ &\leq \left[1 + \frac{L_1}{L_2} K x_{\max} \right] \sum_{k=1}^I \nu(x_k) S_k |f_k - \hat{f}_k| \Delta x_k \\ &\leq \left[1 + \frac{L_1}{L_2} K x_{\max} \right] \max_{x \in (0, x_{\max}]} [\nu(x) S(x)] \sum_{k=1}^I |f_k - \hat{f}_k| \Delta x_k. \end{aligned}$$

Defining, $C = 2[1 + \frac{L_1}{L_2} K x_{\max}] > 0$ and $L_3 := \frac{C}{2}[\max_{x \in (0, x_{\max}]} [\nu(x) S(x)]] < \infty$, we have

$$(4.19) \quad T_1 \leq L_3 \|\mathbf{f} - \hat{\mathbf{f}}\|.$$

Now we consider the second term on the right-hand side of (4.13) for simplification as

$$(4.20) \quad T_2 = \sum_{k=1}^I \left(\frac{\omega_k^b}{x_k} \sum_{j=1}^k x_j \mathcal{B}_{jk} \right) S_k |f_k - \hat{f}_k| \Delta x_k.$$

Using the fact that $x_i \leq x_k \forall i = 1, \dots, k$,

$$(4.21) \quad T_2 \leq \sum_{k=1}^I \frac{\omega_k^b x_k}{x_k} \left(\sum_{j=1}^k \mathcal{B}_{jk} \right) S_k |f_k - \hat{f}_k| \Delta x_k.$$

Changing the order of summation we find

$$(4.22) \quad T_2 \leq \sum_{j=1}^I \sum_{k=j}^I \omega_k^b \mathcal{B}_{jk} S_k |f_k - \hat{f}_k| \Delta x_k = T_1.$$

Hence, we have

$$(4.23) \quad T_2 \leq L_3 \|\mathbf{f} - \hat{\mathbf{f}}\|.$$

Hence, by combining (4.13), (4.19), and (4.23), we have the desired result

$$(4.24) \quad \|\mathbf{J}(\mathbf{f}) - \mathbf{J}(\hat{\mathbf{f}})\| \leq L \|\mathbf{f} - \hat{\mathbf{f}}\|,$$

where $L := 2L_3 < \infty$ is the Lipschitz constant. \square

Next we state the main result of this section.

THEOREM 4.4. *Suppose that the functions S and b are twice continuously differentiable functions over $(0, x_{\max}]$ and $(0, x_{\max}] \times (0, x_{\max}]$, respectively. Then, the solution of the discretization (4.1) is nonnegative and consistent, with a truncation error of the order 2, independently of the type of mesh. Moreover, the method is convergent and the order of convergence is the same as the order of consistency.*

Proof. Here we need to prove three properties of the solution, namely, nonnegativity, consistency, and convergence.

Nonnegativity. Notice that for any $\hat{\mathbf{f}} \in \mathbb{R}^I$ with $\hat{\mathbf{f}} \geq 0$, and $\hat{f}_i = 0$, i.e., for any nonnegative vector $\hat{\mathbf{f}} \in \mathbb{R}^I$ whose i th component equals zero, we have from (4.2) and (4.3)

$$\hat{B}_i(\hat{\mathbf{f}}) \geq 0 \quad \text{and} \quad \hat{D}_i(\hat{\mathbf{f}}) = 0.$$

This signifies that $J_i(\hat{\mathbf{f}})(= \hat{B}_i(\hat{\mathbf{f}}) - \hat{D}_i(\hat{\mathbf{f}})) \geq 0$. This observation is true for any $i = 1, \dots, I$. Then, Theorem 4.1 and Proposition 4.3 readily imply the nonnegativity of the solution.

Consistency. By Definition 1, the i th component of the spatial truncation error is given by

$$(4.25) \quad \sigma_i(t) = \frac{df_i(t)}{dt} - J_i(f_i(t)).$$

Using (3.1) and (4.4), we get

$$(4.26) \quad \sigma_i(t) = (B_i - \hat{B}_i(\mathbf{f})) - (D_i - \hat{D}_i(\mathbf{f})).$$

Let us first evaluate the first term in the parenthesis on the right-hand side. Using (3.8) and (4.2), we find

$$(4.27) \quad B_i - \hat{B}_i(\mathbf{f}) = \frac{1}{\Delta x_i} \left[\sum_{k=i}^I S_k f_k \Delta x_k \mathcal{B}_{ik} - \sum_{k=i}^I \omega_k^b S_k f_k \Delta x_k \mathcal{B}_{ik} \right] + \mathcal{O}(\Delta x^2).$$

Merging the two terms on the right-hand side we obtain

$$(4.28) \quad B_i - \hat{B}_i(\mathbf{f}) = \frac{1}{\Delta x_i} \sum_{k=i}^I (1 - \omega_k^b) S_k f_k \Delta x_k \mathcal{B}_{ik} + \mathcal{O}(\Delta x^2).$$

Now we estimate the term $(1 - \omega_k^b)$ as follows:

$$(4.29) \quad 1 - \omega_k^b = 1 - \frac{x_k \left[\sum_{j=1}^k \mathcal{B}_{jk} - 1 \right]}{\sum_{j=1}^k (x_k - x_j) \mathcal{B}_{jk}} = \frac{x_k - \sum_{j=1}^k x_j \mathcal{B}_{jk}}{\sum_{j=1}^k (x_k - x_j) \mathcal{B}_{jk}}.$$

Using the mass conservation property of the breakage function (1.4), we obtain

$$(4.30) \quad 1 - \omega_k^b = \frac{\sum_{j=1}^k \int_{x_{j-1/2}}^{p_k^j} (x - x_j) b(x, x_k) dx}{\sum_{j=1}^k (x_k - x_j) \mathcal{B}_{jk}}.$$

With the direct application of midpoint and right end quadrature approximations, one can show that the numerator term is of order 2 while the denominator is simply of order 0. Hence, we find that $1 - \omega_k^b = \mathcal{O}(\Delta x^2)$. Thus, (4.28) implies that

$$(4.31) \quad B_i - \hat{B}_i(\mathbf{f}) = \mathcal{O}(\Delta x^2).$$

Proceeding similarly for the second term in the parenthesis on the right-hand side of (4.26), and using (3.9) and (4.3) we get

$$D_i - \hat{D}_i(\mathbf{f}) = (1 - \omega_i^d) S_i f_i + \mathcal{O}(\Delta x^2).$$

Substituting ω_i^d from (3.20), we have

$$(4.32) \quad D_i - \hat{D}_i(\mathbf{f}) = \left(1 - \frac{\omega_i^b}{x_i} \sum_{j=1}^i x_j \mathcal{B}_{ji} \right) S_i f_i + \mathcal{O}(\Delta x^2).$$

Notice that

$$x_i = \int_0^{x_i} xb(x, x_i) dx = \sum_{j=1}^i \int_{x_{j-1/2}}^{x_j} xb(x, x_i) dx = \sum_{j=1}^i x_j \mathcal{B}_{ji} + \mathcal{O}(\Delta x^2).$$

Using x_i in (4.32), we get

$$(4.33) \quad D_i - \hat{D}_i(\mathbf{f}) = (1 - \omega_i^b) \frac{1}{x_i} \left(\sum_{j=1}^i x_j \mathcal{B}_{ji} \right) S_i f_i + \mathcal{O}(\Delta x^2).$$

Using the fact that $1 - \omega_k^b = \mathcal{O}(\Delta x^2)$, we have

$$(4.34) \quad D_i - \hat{D}_i(\mathbf{f}) = \mathcal{O}(\Delta x^2).$$

Hence, (4.26), (4.31), and (4.34) follow

$$(4.35) \quad \sigma_i(t) = \mathcal{O}(\Delta x^2) \Rightarrow \|\boldsymbol{\sigma}(t)\| = \mathcal{O}(\Delta x^2).$$

Convergence. Theorem 4.2, Proposition 4.3, and the above result on consistency prove that the proposed method converges and the order of the convergence is the same as the order of consistency. \square

Remark 2. It can be followed from the work of Dubovskii and Stewart [3] that the smoothness of the kernels b and S implies the smoothness of the number density function f . In this work the functions b and S are assumed to be twice continuously differentiable and so is the density function f .

5. Numerical validation. To validate the proposed method, numerical results are compared against several test cases. In particular, the first two test cases have known analytical solutions whereas the third test case is more practically oriented and does not possess an exact solution. The exact solutions of the number density distribution for the first two test cases can be found in Singh, Saha, and Kumar [17] and Ziff and McGrady [19].

Both uniform and nonuniform meshes are considered for validation. The nonuniform meshes are generated with the rule $x_{i+1/2} = rx_{i-1/2}$ for some real number $r > 1$. The maximum and minimum sizes of the computational domain are taken to be 1 and 10^{-8} , respectively. In order to know the extent of breakage in numerical computations, it is convenient to express the zeroth moment in a dimensionless form. The extent of breakage, a dimensionless form of the zeroth moment, is defined as $\mu_0(t)/\mu_0(0)$, where $\mu_0(t)$ is the zeroth moment of the distribution at time t . The value of the extent of breakage mentioned in this work is reached at the final time of computation. For the integration of the discrete system (4.1), the MATLAB ODE45 solver is used.

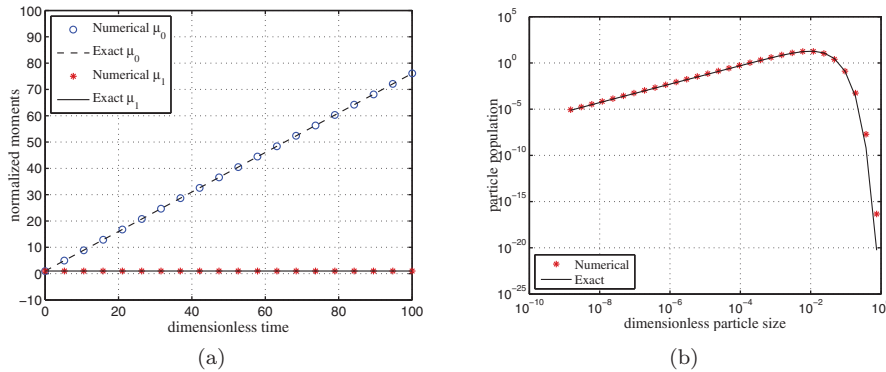


FIG. 2. A comparison of numerical results of test case I.

The comparisons are based on a number of features including different normalized moments as well as particle size distribution. Normalization of moments is done by dividing the values at different times by the initial value of the moment. The mathematical results of convergence analysis are also validated numerically in all three test cases on uniform as well as on nonuniform meshes. The experimental (numerical) order of convergence (EOC) and relative error are calculated as in Kumar and Warnecke [7, 8] as well as Kumar and Kumar [9]. For the case of known exact results, some additional comparisons are performed to assess the accuracy of numerical results to predict the first two moments and the particle size distribution.

5.1. Test case I. We begin the validation process with a simple example of binary breakage. We consider a problem of uniform binary breakage function $b(x, y) = 2/y$ and linear selection function $S(x) = x$ taking monodisperse particles of size unity as initial condition. Notice that this is the same test case as considered earlier in section 2. Figure 2 shows the numerical results of the first two moments and particle population in different cells. The computation is carried out for a large extent of breakage $\mu_0(t)/\mu_0(0) \approx 100$ which corresponds to the dimensionless time $t = 100$. The computational domain is divided into 30 nonuniform cells of the type described above.

The prediction of zeroth and first moments is shown in Figure 2(a). The results follow very closely the true values. In Figure 2(b), the particle population of each cell is plotted against the representative size of the respective cell. These numerical results are slightly overpredictive at large particle sizes. Overall, the degree of accuracy is quite high. It is important to notice by comparing Figures 1 and 2 that the drawback of the finite volume scheme of Kumar and Kumar [9] is overcome. Moreover, the CPU time taken by a desktop computer to run the simulation is comparable to that of Kumar and Kumar [9]. Table 1 summarizes numerical results of relative error along with the order of convergence. To support applicability of the method for different meshes, we obtain these results for uniform as well as nonuniform meshes. As expected, the results clearly show the convergence of order 2, independently of the meshes.

5.2. Test case II. Test case II is similar to the previous test case. The only difference lies in the choice of the selection function. The selection function for this test case is taken to be quadratic, i.e., $S(x) = x^2$. The computational domain is divided into 60 nonuniform cells. The computation is carried out up to $t = 100$ that correlates to an extent of breakage $\mu_0(t)/\mu_0(0) \approx 18$. All other simulation conditions remain the

TABLE 1
Experimental order of convergence for test case I.

(a) Uniform grids			(b) Nonuniform grids		
Grid points	Relative error L_1	EOC	Grid points	Relative error L_1	EOC
30	0.4669	-	30	0.057	-
60	0.2249	1.0540	60	0.0146	1.8573
120	0.0816	1.4623	120	0.0037	1.9615
240	0.0247	1.7253	240	0.0009	1.9902
480	0.0068	1.8665	480	0.0002	1.9974

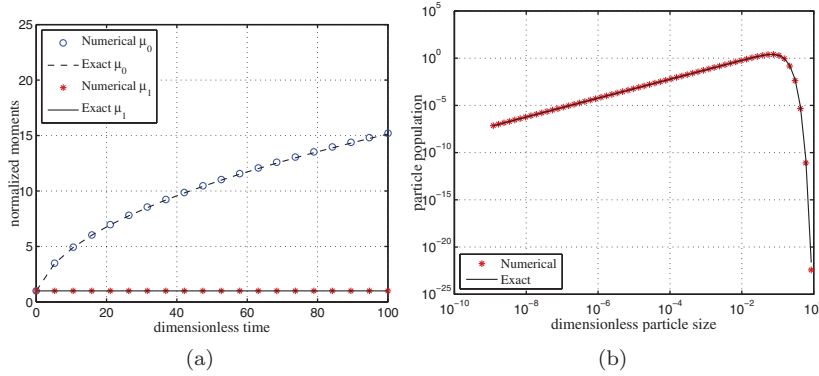
FIG. 3. *A comparison of numerical results of test case II.*

TABLE 2
Experimental order of convergence for test case II.

(a) Uniform grids			(b) Nonuniform grids		
Grid points	Relative error L_1	EOC	Grid points	Relative error L_1	EOC
60	0.0047	-	60	0.0210	-
120	0.0012	1.9130	120	0.0053	1.9921
240	0.0003	1.9559	240	0.0013	1.9940
480	0.0001	1.9768	480	0.0003	1.9993

same. Computation in this case is more difficult than in the earlier case because of the stronger size dependency in the selection function. Figure 3(a) compares results of zeroth and first moments. Once again, temporal change of the zeroth moment is well captured by the numerical method. As expected, results of first moment remain constant with time and follow closely their true values. Clearly, the numerical results of particle population by the proposed method are highly accurate as shown in Figure 3(b). The numerical results of the order of convergence and relative error are shown in Table 2. Once again, these results support the mathematical analysis that the method is of order 2 and the order does not depend on the type of mesh.

5.3. Test case III. The validation is completed by taking a more complex test case, the exact solution of which is not known. We consider a problem with the following breakage and selection functions,

$$b(x, y) = \frac{12x}{y^2} \left(1 - \frac{x}{y}\right), \quad S(x) = x^2,$$

TABLE 3
Experimental order of convergence for test case III.

(a) Uniform grids			(b) Nonuniform grids		
Grid points	Relative error L_1	EOC	Grid points	Relative error L_1	EOC
60	-	-	60	-	-
120	0.0311	-	120	0.2756	-
240	0.0085	1.8757	240	0.0624	2.1426
480	0.0022	1.9595	480	0.0154	2.0167
960	0.0006	1.8633	960	0.0039	2.0016

along with the following normally distributed initial condition

$$f(x, 0) = \frac{1}{\sigma\sqrt{2\pi}} \exp\left[-\frac{(x - \mu)^2}{2\sigma^2}\right], \quad \sigma^2 = 0.01, \mu = 0.5.$$

The computation is performed until $t = 200$, corresponding to the extent of breakage $\mu_0(t)/\mu_0(0) \approx 12$. In this case, only numerical results of order of convergence are computed. To calculate the error and the experimental order of convergence we refer to Kumar and Warnecke [7]. Table 3 clearly shows that the proposed method is second order accurate and the order of the method does not depend on the type of mesh.

6. Conclusions. In this study, a new approach based on a finite volume method has been presented for solving the breakage PBE on nonuniform meshes. The proposed method is simple to code and computationally very efficient. A complete mathematical analysis has been performed that proves that the method is second order convergent. Moreover, it has been shown that the method conserves the total mass of the system and predicts the temporal evolution of the zeroth moment with high accuracy. Furthermore, all observations have been verified numerically against several test problems. The new method produces very accurate results using only a few grid points. The numerical results show the ability of the new method to predict very well the time evolution of the zeroth moment as well as the complete particle size distribution. The numerical order of convergence confirms the theoretical observations that the method is second order convergent and the convergence rate does not depend on the type of mesh.

Acknowledgment. The authors would like to thank Otto-von-Guericke University, Magdeburg, Germany for their hospitality during this work.

REFERENCES

- [1] J.P. BOURGADE AND F. FILBET, *Convergence of a finite volume scheme for coagulation-fragmentation equations*, Math. Comp., 77 (2008), pp. 851–882.
- [2] P.B. DUBOVSKIĬ, V.A. GALKIN, AND I.W. STEWART, *Exact solutions for the coagulation-fragmentation equation*, Math. Methods Appl. Sci., 25 (1992), pp. 4737–4744.
- [3] P.B. DUBOVSKIĬ AND I.W. STEWART, *Existence, uniqueness and mass conservation for the coagulation-fragmentation equation*, J. Phys. A, 19 (1996), pp. 571–591.
- [4] F. FILBET AND P. LAURENÇOT, *Numerical simulation of the Smoluchowski coagulation equation*, SIAM J. Sci. Comput., 25 (2004), pp. 2004–2028.
- [5] L. FORESTIER-COSTE AND S. MANCINI, *A finite volume preserving scheme on nonuniform meshes and for multidimensional coalescence*, SIAM J. Sci. Comput., 34 (2012), pp. B840–B860.
- [6] W. HUNDSDORFER AND J.G. VERWER, *Numerical Solution of Time-Dependent Advection-Diffusion-Reaction Equations*, Springer Ser. Comput. Math. 33, 2003, pp. 215–323.

- [7] J. KUMAR AND G. WARNECKE, *Convergence analysis of sectional methods for solving breakage population balance equations - I: The fixed pivot technique*, Numer. Math., 111 (2008), pp. 81–108.
- [8] J. KUMAR AND G. WARNECKE, *Convergence analysis of sectional methods for solving breakage population balance equations - II: The cell average technique*, Numer. Math., 110 (2008), pp. 539–559.
- [9] R. KUMAR AND J. KUMAR, *Numerical simulation and convergence analysis of a finite volume scheme for solving general breakage population balance equations*, Appl. Math. Comput., 219 (2013), pp. 5140–5151.
- [10] W. LAMB, *Existence and uniqueness results for the continuous coagulation and fragmentation equation*, Math. Methods Appl. Sci., 27 (2004), pp. 703–721.
- [11] P. LAURENÇOT, *On a class of continuous coagulation-fragmentation equations*, J. Differential Equations, 167 (2000), pp. 245–274.
- [12] P. LINZ, *Convergence of a discretization method for integro-differential equations*, Numer. Math., 25 (1975), pp. 103–107.
- [13] D.J. McLAUGHLIN, W. LAMB, AND A.C. MCBRIDE, *A semigroup approach to fragmentation models*, SIAM J. Math. Anal., 28 (1997), pp. 1158–1172.
- [14] D.J. McLAUGHLIN, W. LAMB, AND A.C. MCBRIDE, *An existence and uniqueness result for a coagulation and multiple-fragmentation equation*, SIAM J. Math. Anal., 28 (1997), pp. 1173–1190.
- [15] D. RAMKRISHNA, *Population Balances. Theory and Applications to Particulate Systems in Engineering*, Academic Press, New York, 2000.
- [16] J. SAHA AND J. KUMAR, *The singular coagulation equation with multiple fragmentation*, Z. Angew. Math. Phys., 66 (2015), pp. 919–941.
- [17] R. SINGH, J. SAHA, AND J. KUMAR, *Adomian decomposition method for solving fragmentation and aggregation population balance equations*, J. Appl. Math. Comput., 48 (2015), pp. 265–292.
- [18] R.M. ZIFF, *New solutions to the fragmentation equation*, J. Phys. A, 24 (1991), pp. 2821–2828.
- [19] R.M. ZIFF AND E.D. McGRADY, *The kinetics of cluster fragmentation and depolymerisation*, J. Phys. A, 18 (1985), pp. 3027–3037.